12 Additional Information for Fracture Assessment

12.1 Local approach

12.1.1 Introduction

Local approach methods are based on the application of micro-mechanical models of failure in which the stress, strain and 'damage' local to a crack tip or stress concentration are related to the critical conditions required for fracture. Each model contains several material-specific parameters that are calibrated using a combination of reference test data, quantitative metallography and finite element analysis. Once the parameters have been derived for a particular material they can be assumed to be independent of geometry and loading mode and may therefore be transferred to the assessment of any structure fabricated from the same material.

Local approach models have been the subject of significant development, being used to predict the fracture behaviour of both ferritic and austenitic steel structures for a range of geometries under combinations of primary and secondary load [12.1-12.5]. The results show that local approach methods provide an alternative, though complementary approach to the fracture mechanics methods described in Section 6. When used in component assessments, they automatically address the effects of load-history (Section 6.2.3.9), constraint (Section 6.2.3.10) and weld mismatch (Section 6.2.3.11). As the methods use detailed finite element analysis, separate calculations of stress intensity factor and limit load are not needed. The methods may also be used to derive fracture toughness data, for example to predict or interpolate the effects of constraint on fracture toughness to aid application of the methods of Section 6.4.3.

Local approach methods are not described in detail here. Instead, a brief description of some models and a procedure for their application is given in Sections 11.6.2 and 11.6.3, respectively. Finally, Section 11.6.4 contains a discussion of some of the limitations of the approach.

12.1.2 Models

There are a number of local approach models including the Beremin cleavage fracture model [12.6], the Beremin ductile fracture model [12.7], the Rousselier damage mechanics model [12.8], and the Gurson damage mechanics model [12.9]. The first model is a cleavage fracture model and the remaining three are ductile damage models. In this section, a single cleavage model (Beremin) and a single ductile model (Gurson) are described for illustration. More detailed information on these and other models and their application is contained in Section III.9 of R6 [12.10].

12.1.2.1 Beremin model of cleavage

The Beremin model of cleavage uses a two-parameter Weibull description of the cumulative failure probability, P [12.6]:

$$P = 1 - \exp\left\{-\left(\sigma_W / \sigma_u'\right)^m\right\} \tag{12.1}$$

where σ_W is the Weibull stress, m is the Weibull shape parameter and σ_u' is a characteristic stress. Both m and σ_u' are material parameters. The Weibull stress is defined by the following summation over all finite elements, j, within the plastic zone,

$$\sigma_W = \left\{ \sum_{\mathrm{j\ in\ pz}} \sigma_{1,j}^{m} (\Delta V_j / V_u) \right\}^{1/m} \tag{12.2}$$

where $\sigma_{1,j}$ is the maximum principal stress in the j'th element, of volume ΔV_j, in the plastic zone. The parameter V_u is a characteristic volume related to the materials microstructure. The probability of fracture can be determined by post-processing the results for the maximum principal stress and the plastic zone size from a standard elastic-plastic finite element analysis.

12.1.2.2 Gurson Damage Mechanics Model

Gurson modelled the ductile failure process by constitutive equations which represent the mechanical properties of the material as damage evolves. The plastic potential F which controls plastic straining is defined by

$$F = \left(\sigma_{eq} / \sigma_M\right)^2 + 2q_1 f \cosh\left(3q_2\sigma_m / (2\sigma_M)\right) - \left(1 + q_3 f^2\right) = 0 \tag{12.3}$$

where σ_{eq} is the equivalent stress, σ_m is the hydrostatic stress, σ_M is the equivalent stress from the conventional stress-strain curve as a function of equivalent plastic strain and f is the current void volume fraction. The factors q_1, q_2 and q_3 are material parameters. A model describing void initiation and growth is also required to determine f and failure is taken to correspond to a critical value of f. The model modifies the constitutive equations used to describe material flow behaviour by incorporating the effects of damage (f) and a specialist finite element code or standard codes incorporating user-defined material behaviour are required for its application.

12.1.3 Procedure

The use of local approach models to predict structural behaviour follows the following steps.

Step 1: Obtain reference experimental data for the material of interest. Reference data should relate to the fracture mode of interest and preferably be obtained from pre-cracked specimens which span the crack-tip constraint level of the structural application and are tested at temperatures close to that of interest.

Step 2: Based on microstructural considerations and the reference data, estimate the parameters for the local approach model of interest.

Step 3: Perform appropriate finite element analyses of the reference experiments and compare the predicted specimen behaviour with that observed in the reference experiments.

Step 4: If the comparison in Step 3 is outside the accuracy required for the model of interest, adjust the model parameters and repeat Steps 2 and 3 as appropriate.

Step 5: Once the comparison performed in Step 3 is sufficiently accurate, structural behaviour may be predicted by using the model parameters in a finite-element analysis of the structure of interest.

Step 6 Perform analyses to demonstrate that the results are not sensitive to variations in inputs such as the local approach parameters. For example, the range of parameters considered should be sufficient to predict a fracture toughness corresponding to the lower bound toughness which would be used in the procedure of Section 6.

12.1.4 Discussions and Limitations

Attempts to use local approach methods to predict cleavage fracture following tearing in the transition temperature regime has been made with some success [12.11], but the methods are not yet well established.

The procedures for application of local approach models to three-dimensional situations are less standardised than those for axisymmetric, plane stress and plane strain finite element analyses. For three-dimensional applications, such as finite-length surface or buried defects, careful consideration needs to be given to the refinement of crack-tip elements in the out-of-plane dimension.

Within the Beremin model of cleavage fracture, various definitions of the Weibull stress are being developed to quantify possible biaxial load effects on fracture. In equation (12.1), a formulation of σ_W based on the distribution of maximum principal stress within the plastic zone has been adopted since this is the most widely used. However, other formulations are under development.

12.1.5 Bibliography

[12.1] D Miannay, Mecanique de la rupture, Les Editions de Physique, France (1995).

[12.2] C S Wiesner, The ‘local approach’ to cleavage fracture, Woodhead Publishing Limited, Cambridge, UK (1995).

[12.3] A Pineau, Review of fracture micromechanisms and a local approach to predicting crack resistance, Advances in Fracture Research, 5th International Conference on Fracture, Ed. D Francois, 2, 553-577 (1981).

[12.4] A H Sherry and D P G Lidbury, Application of local approach to the measurement of fracture toughness in the transition temperature range, AEA Technology Report AEA-TRS-4092 (1991).

[12.5] D P G Lidbury, A H Sherry, B A Bilby, I C Howard, Z H Li and C Eripret, Prediction of the first Spinning Cylinder test using continuum damage mechanics, Nucl Engng Design 152, 1-10 (1994)

[12.6] F M Beremin, A local criterion for cleavage fracture of nuclear pressure vessel steels, Met Trans 14A, 2277-2287 (1983).

[12.7] F M Beremin, Experimental and numerical study of the different stages in ductile rupture: Application to crack initiation and stable crack growth, Three-dimensional constitutive relations and ductile fracture, Ed. S Nemat-Nasser, North Holland Publishing Company, 185-205 (1981).

[12.8] G Rousselier, Ductile fracture models and their potential in local approach of fracture, Nucl Engng Design 105, 97-111 (1987).

[12.9] A L Gurson, Continuum theory of ductile rupture by void nucleation and growth: Part I - Yield criteria and flow rules for porous ductile materials, ASME J Engng Mater Techol 99, 2-15 (1977).

[12.10] Assessment of the Integrity of Structures Containing Defects, Proceudre R6 Revision 4, British Energy, Gloucester (2005).

[12.11] A H Sherry, D Beardsmore, D P G Lidbury, I C Howard and M A Sheikh, Remnant life assessment using the local approach; a prediction of the outcome of the NESC experiment, HSE Seminar on Remnant Life Prediction, Institution of Mechanical Engineers, London, 26 November (1997).

12.2 Thin walled structures

12.2.1 Introduction

With respect to flaw assessment, thin wall structures show some special features, which are not, or only partially, covered by the method in the main body of this procedure. These are:

• pronounced stable crack extension prior to failure,

• constraint and other issues which make any application of standard test methods for fracture toughness impossible or too conservative,

• buckling as a failure mechanism competitive to fracture.

12.2.2 Pronounced Stable Crack Extension Prior to Failure

It is common knowledge that crack driving force parameters such as the J-integral cannot be applied to pronounced stable crack extension. On the other hand the crack tip opening angle (CTOA) or displacement (CTOD) parameters are well suited for modelling stable crack extension as well as fracture instability, see the overview in [12.12]. The procedure in the main body of this document offers the application of the CTOD for assessment purposes but it gives it in general terms only. In contrast to this, the CTOD-δ_5 parameter [12.13] is used as a specific definition for thin walled structures in this option. Fig. 12.1 shows the basic arrangement for the experimental determination of δ_5. The CTOD-δ_5 parameter offers the possibility for determining the toughness and the crack driving force in a direct way by measuring or calculating the relative displacement of two gauge points which are located 5 mm apart on a straight line going through the original pre-crack tip. This definition has a number of advantages:

• There is a unique definition for laboratory specimens and components.

• Usually, conventional CTOD values cannot be determined at all for thin sheet materials because the geometry of the semi-finished products does not meet the thickness requirements of the test standards. Performing the test on thicker sheets is also not possible when the material is manufactured by rolling because that process alters its mechanical properties.

• The drawback of measuring the displacement at the specimen surface usually does not matter significantly for thin sheets. Due to the location of the gauge points, each 2.5 mm apart from the original crack tip, the CTOD-δ_5 averages displacement through the wall thickness.

• The most important advantage is that the CTOD-δ_5 is particularly suited for correlating stable crack extension. It has been demonstrated that δ_5 is able to correlate large amounts of crack extension [12.13]. δ_5 is uniquely correlated with the crack tip opening angle [12.12,12.17].

12.2.3 Low Constraint Fracture Toughness

Thin sheet materials can usually not be tested on the basis of the available fracture mechanics test standards. This is the background of ISO and ASTM standardisation activities initiated in 1998, with the aim of providing test methods for low constraint specimens such as thin sheets [12.14]. The methods are mainly based on the CTOA and CTOD-δ_5 parameters. The constraint issue is addressed by two conditions.

• The specimen thickness, B, has to be chosen identical to that of the component or the semi-finished product in order to provide identical out-of-plane constraint and material conditions.

• As shown by several studies [12.12,12.16, 12.21, 12.22 and 12.23] R-curves for some materials, typically used for thin sheet materials, such as aluminium alloys, tend to be independent of the in-plane dimensions of the specimen or component if the crack length, a, and the uncracked ligament length, W-a, are greater than about four times the thickness, B:

$$a / B \text{ and } (W - a) / B \geq 4 \tag{12.4}$$

Real thin wall components will usually meet this condition, which in many cases ensures geometry independent R-curves as long as stable crack extension does not exceed a value of

$$\Delta a_{max} = \begin{cases} 0.25\,(W - a_o) & C(T) \text{ and } SE(B) \text{ specimens} \\ W - a_o - B & M(T) \text{ specimens} \end{cases} \tag{12.5}$$

12.2.4 Buckling as a Failure Mechanism Competitive to Fracture

The only competing failure mechanism the FITNET procedure offers in its main body is plastic collapse which is covered by the $L_{r\ max}$ criterion in Section 6. Besides this, other failure mechanisms such as plastic deformation, wear, or cavitation may cause a structure to loose its functionality. In the case of thin wall structures buckling is an important failure mechanism which has to be taken into account.

12.2.5 The Procedure

The present thin wall option was validated by a number of experiments on M(T) plates with and without welds (laser beam and friction stir welded Al-alloys of aerospace grade) and bi-axially loaded cruciform specimens subjected to mode I and mixed mode loading made of various aluminium alloys and ferritic and austenitic steels. It is restricted to simple thin walled geometries without stiffeners.

It follows the Analysis Options 1 and 3 procedures (such as given in 6.3.2 and 6.3.4) but added by a number of specific items:

• The general equations 6.1-6.3 are used in combination with the specific CTOD-δ_5 definition (Fig. 12.2).

• The Analysis Option 1 and the Analysis Option 3 $f(L_r)$ functions are applied as given by Equations 6.38-6.45 in 6.3.

• Since thin plates are manufactured by rolling, they may tend to anisotropy in their tensile properties. The deformation pattern at the crack tip is three-dimensional and, as a consequence, not adequately characterised by the tensile test results. In order to avoid non-conservatism it is recommended to base the SINTAP analyses on the lowest stress-strain curve.

• The applied load-stable crack extension characteristic can be determined as illustrated in Fig 12.2 which gives an example of the CDF philosophy.

• The δ_5-R-curve as the toughness input parameter has to be obtained on specimens exhibiting a thickness, B, identical to the component to be assessed and a crack length, a, and an initial uncracked ligament length, W-a, equal or greater than four times the thickness, B (Eq. 12.4).

It was already mentioned that R-curves tend to be independent of the specimen or component dimensions when this requirements are fulfilled. Note, however, that this statement cannot be generalised. Therefore, geometry independence of the R curve has to be checked when the method is applied to new materials. In cases where no geometry independency is stated, the lowest R-curve has to be used which is usually obtained from C(T) specimens.

• The validity limits of the δ_5 concept have to be met (Eq. 12.5).

• In order to avoid extrapolation of the δ_5-Δa curve beyond its validity limits the stable crack extension Δa at the maximum load in the component as an output of the analysis should not exceed the Δa range which is covered by the experimental R-curve. As a rule, the width W of C(T) type test specimens should not be smaller than about 150 mm.

• The treatment of the mixed mode effect follows Section11.5 of the present procedure.

Note 1: *Mixed mode cracks which are not affected by features like weldments, notches or geometrical transitions tend to change their growth direction after a certain amount of extension. This amount refers to factors such as the global mixed mode ratio and the ductility of the material. According to [12.19] (see also the discussion in [12.20, App. 1] the effect is more distinct in brittle than in ductile materials. This means with respect to the procedure proposed in this paper that, in principle, the analysis should be done for both, the mixed mode crack and the Mode I crack. The lower maximum load should then be chosen as the final result.*

Note 2:*: At present, the procedure is mainly validated for plane geometries. Limited amount of work has been carried out for the panels with laser beam welded stiffeners (see. 12.22 and 12.23). Further application and validation of the procedure is presented at the FITNET 2006 Conference. If it is applied to curved panels such as fuselages and other pressure vessel, both, K factor and yield load solutions as input parameters to the analysis have to be chosen which take explicitly into account bulging effects. The same might be true for plane components subjected to bending or local buckling at the crack. For plane bending geometries which large ligament sizes the available global limit load solutions are not appropriate and may yield an overestimation of the load carrying capacity.*

Note 3: *Present section is strongly linked with the damage tolerance behaviour of aerospace structures (see Section 14, Tutorials) and this section will be included into that part during the next revision.*

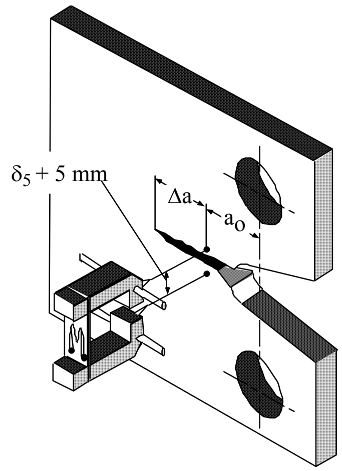

Figure 12.1 Definition and experimental determination of the CTOD-δ_5 parameter

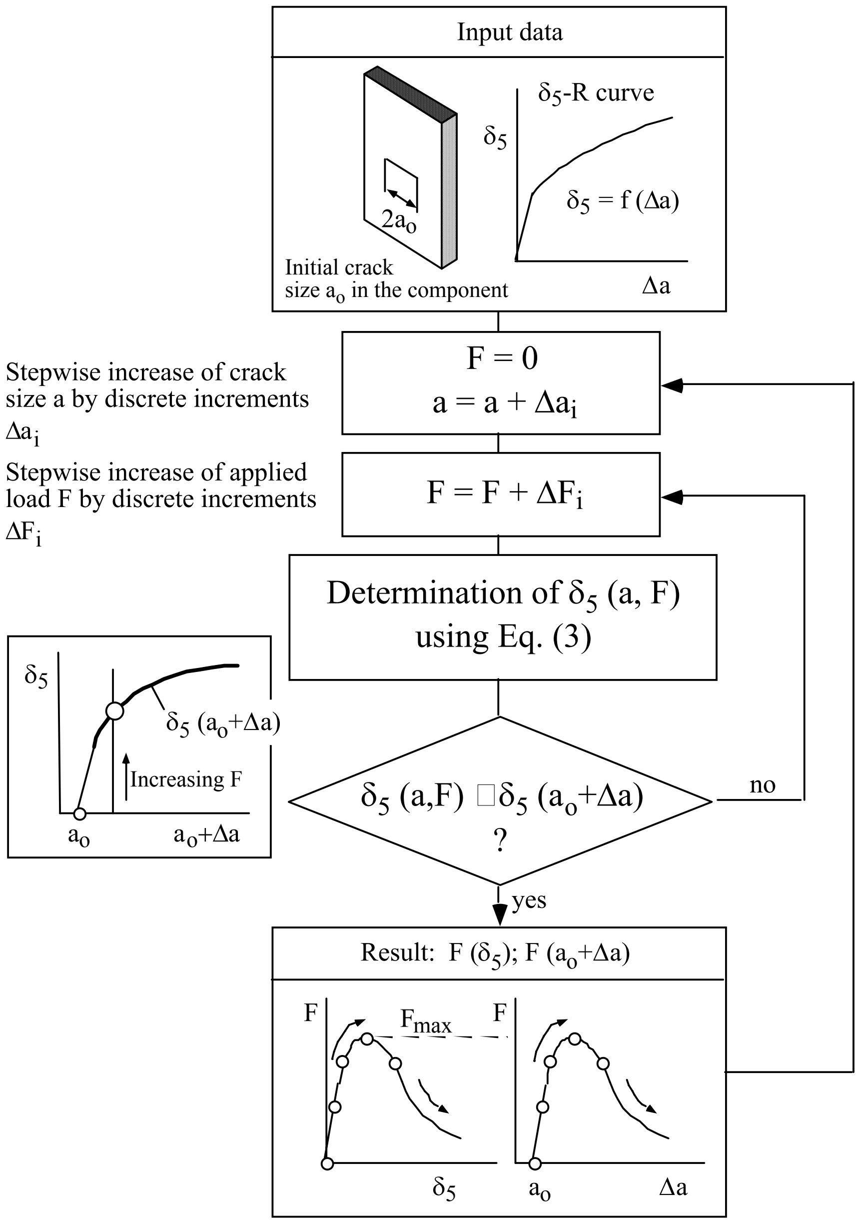

Figure 12.2 Flow chart for the determination of the applied load-δ_5 and applied load-stable crack extension characteristics. The determination follows the Crack Driving Force (CDF) philosophy.

12.2.6 Bibliography

[12.12] Newman JC Jr., James MA, Zerbst U. A review of the CTOA/CTOD fracture criterion. Engineering. Fracture Mechanics, v.70, N.3-4, 2003, pp. 371-385

[12.13] Schwalbe K.-H. Introduction of d5 as an operational definition of the CTOD and ist practical use. ASTM STP 1256, 1995: 763-78, American Society for Testing and Materials, West Conshohocken.

[12.14] Draft International Standard ISO/DIS 22889. Metallic Materials – Method of Test for the Determination of Resistance to Stable Crack Extension Using Specimens of Low Constraint, 2005.

[12.15] Schwalbe K-H, Heerens J, Zerbst U, Koçak M. EFAM-GTP 02, The GKSS Procedure for Determining the Fracture Behaviour of Materials, Second Edition., GKSS Research Centre Geesthacht, Geesthacht, 2002.

[12.16] Heerens J, Schwalbe K-H. R-curve testing and its relevance to structural assessment. Fat. Fract. Engng. Mat. Struct. 1998; 21: 1259-1271

[12.17] Schödel, M. and Zerbst, U. (2004): Application of the European flaw assessment procedure SINTAP to thin wall structures. Analytical assessment levels. Engineering Fracture Mechanics 71, 1035-58

[12.18] Schödel, M. and Zerbst, U. (2005): Application of the European flaw assessment procedure SINTAP to thin wall structures subjected to biaxial and mixed mode loading. Under preparation

[12.19] Dalle Donne C. Übertragbarkeit von Risswiderstandskurven von Standardproben auf biaxial belastete, bauteilähnliche Kreuzproben. Fortschr.-Berichte VDI, Series 18, No. 205, 1997, VDI-Verl., Düsseldorf

[12.20] Dalle Donne C. The crack tip displacement vector approach to mixed-mode fracture. ASTM STP 1359, 21-40, American Society for Testing and Materials, West Conshohocken,1999.

[12.21] Kocak M, Seib E, Motarjemi A, Improvements to the fracture assessment of welds using FITNET fitness-for-service assessment procedure, Proc. Int. Conf. OMAE 2005, Halkidiki, Greece, 12-17 June 2005, ASME.

[12.22] Seib E and Kocak M, Fracture analysis of strength undermatched welds of thin-walled aluminium structures using FITNET Procedure, Welding in the world, Vol. 49, No. 11/12-2005, pp. 58-69.

[12.23] Seib E. Residual strength analysis of laser beam and FSW welded aluminium panels for aerospace applications, PhD Thesis, Dec. 2005, TUHH, Germany, also GKSS 2006/3.

12.3 Loading Rate Effects on Fracture Toughness

12.3.1 Introduction

In certain fracture problems, time becomes an important variable. At high loading rates, two phenomena affect and complicate the evaluation of dynamic fracture toughness of metallic materials:

→ rate-dependent material behaviour (for most metals, flow stress can increase appreciably when strain rate increases by several orders of magnitude);

→ inertia effects, which are of importance when force changes abruptly or the crack grows rapidly (a portion of the work applied to the specimen is converted to kinetic energy).

The rate of material deformation near the crack tip usually is measured as $\dot{K} = dK_I / dt$. For loading rates up to $\dot{K}$ = 10^6 MPa√m/s (such as those which will be addressed in this chapter), in most cases the first and partially the second effect become significant and have to be taken into account when measuring fracture toughness, while the third effect might be neglected.

The consequence of an increase in loading rate on fracture toughness can be schematically outlined as follows, as a function of the fracture regime where the material is expected to operate:

→ <u>brittle fracture behaviour (lower shelf)</u>: an increase in loading rate produces a decrease of fracture toughness (i.e. $K_{Id} < K_{Ic}$);

→ <u>ductile-to-brittle transition regime</u>: the temperature which corresponds to the transition from mainly brittle to mainly ductile behaviour increases with increasing loading rate (i.e. $T_{o,dyn} > T_{o,st}$);

→ <u>ductile fracture behaviour (upper shelf)</u>: increasing the loading rate tends to improve the material's resistance to ductile crack initiation and propagation (i.e. $J_{Id} > J_{Ic}$).

In graphical terms, the effects of an increase in loading rate on the whole fracture toughness vs temperature transition curve of a ferritic steel can be represented as in Figure 12.3.

12.3.2 Experimental Determination of Fracture Toughness at High Loading Rates

The official and most commonly used test standards for fracture toughness determination (ASTM, BS and ISO) mainly address a range of loading rates which goes under the general denomination of "static" or "quasi-static". Some of them, but

not all, include provisions for higher loading rates. The only fracture toughness test standard dealing solely with high loading rates is the third part of BS 7448 [12.21]. BS 7448 - Part 3 describes a method for the determining the opening mode plane strain fracture toughness K_{Ic}, the critical crack tip opening displacement (CTOD) fracture toughness and the critical J fracture toughness of metallic materials for the rates of increase in stress intensity factor greater than 3.0 MPa√m/s but less than 3000 MPa√m/s during the initial elastic deformation. Nevertheless, Annex A of BS 7448-Part 3 gives the recommendations on the determination of fracture toughness in cases when the rate of change in stress intensity factor exceeds 3000 MPa√m/s, provided that the test duration is not less than 1 ms.

However, none of the existing standards, at present, specifically deal with measuring fracture toughness from pre-cracked Charpy-type specimens tested with an instrumented impact pendulum; and this, in spite of the relative popularity of such a test within the scientific community.

In the following, we will try to provide guidelines for obtaining fracture toughness values at loading rates above the quasi-static range in the different fracture regimes (lower shelf, transition and upper shelf).

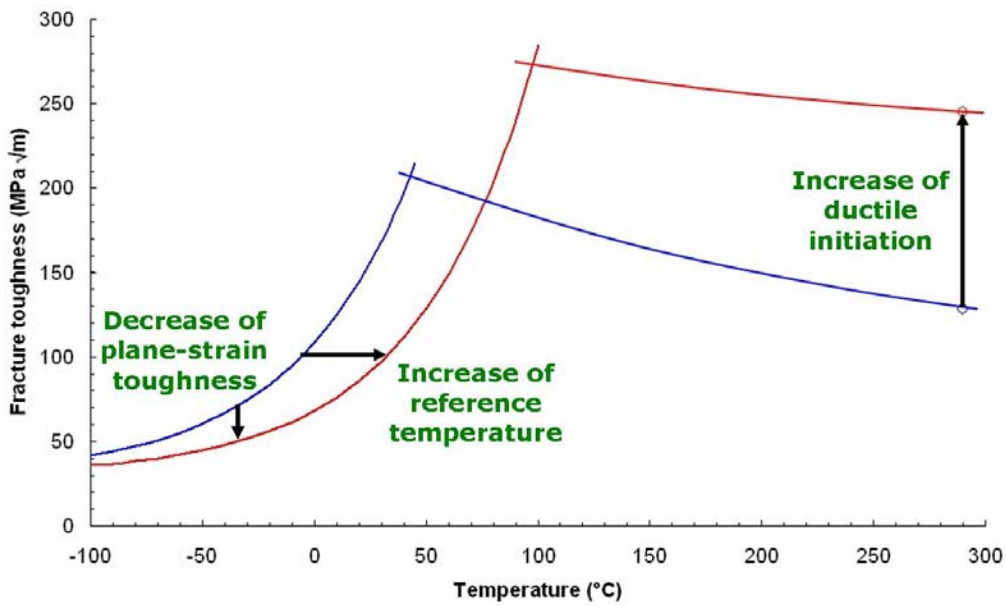

Figure 12.3 - Qualitative effect of increasing loading rate on fracture toughness of ferritic steels (blue curve: quasi-static loading rates; red curve: dynamic loading rates).

12.3.3 Lower Shelf and Early Transition Region (Mainly Brittle Behaviour)

Both ASTM E399 [12.22] and ASTM E1820 [12.23] prescribe that tests be conducted at a rate such that the rate of increase of stress intensity is within the range 0.55 to 2.75 MPa√m/s in the linear elastic region while ISO Unified Test method 12135:2002 [12.24] allows slightly higher rate of increase of stress intensity factor (3.0 MPa√m/s). Above these ranges (rapid-load plane-strain fracture toughness testing), the following provisions are given in BS 7448 - Part 3, ASTM E399 (Annex A7) and ASTM E1820 (Annex A13):

→ force/deflection, force/time and deflection/time curves shall be analysed to ensure that the force values needed to evaluate K_{Ic} (such as P_Q) can be unambiguously determined;

→ the test time *t*, corresponding to the time needed to reach P_Q or K_Q, shall not be less than 1 ms and shall be used as a subscript for the test result, $K_{Ic}(t)$;

→ the yield strength of the material, determined or estimated for the appropriate loading rate, shall be used for the analysis of the fracture test data.

All other requirements and prescriptions for static K_{Ic} determination remain applicable, including preparation of test specimens and validity criteria.

ASTM E399 and ASTM E1820 standards explicitly exclude impact or quasi-impact testing (free-falling or swinging masses) and state that "*substantial decreases in toughness may be noted as the loading rate increases*".

- ***Testing of precracked Charpy-type specimens using an instrumented pendulum***

As previously mentioned, no official test standard presently exists for this kind of tests, neither at ASTM nor at ISO level.

We will therefore refer, in this chapter, to the latest draft version of a Test Procedure developed by the ESIS Technical Sub-Committee 5 (TC5) [12.25]. This document can be considered a useful compendium of experimental and analytical approaches to dynamic toughness tests performed on Charpy-type specimens using an instrumented pendulum.

When the material response is essential linear-elastic, a quasi-static evaluation of the critical fracture toughness in accordance with ISO 12135:2002, based solely on the force value corresponding to cleavage, is allowed only provided a minimum of 5 oscillations are recorded up to fracture or if their amplitude is small compared to the mean value at fracture. This ensures sufficient damping of inertia effects on the force/displacement trace before the occurrence of fracture. Otherwise, the following dynamic evaluation methods are recommended.

→ Impact Response Curve [12.26] and Dynamic Key Curve [12.27] methods, which both require an accurate evaluation of the time to fracture t_f, to be used in a sort of key curve-type methodology. For the determination of t_f, commonly used methods include:

  - strain-gageing the specimen close to the crack tip, which allows identifying the onset of crack extension by a sudden drop of the strain-gage signal;

  - placing a magnetic sensor (e.g. a coil) close to the crack tip and identifying fracture by a magnetic signal recorded by the sensor.

→ Crack Tip Strain Gauge method, which requires positioning a small strain gauge close to the crack tip (as mentioned above) and deriving the value of force at fracture by means of a calibration curve, previously obtained by statically loading the specimen up to the maximum force applied during fatigue precracking [12.28].

Although numerical modelling (i.e. through the use of finite element methods) can also be used to determine the variation of DSIF (Dynamic Stress Intensity Factor) with time (especially for extremely short-time tests as one-point bending [12.29]), simpler methods like modal superposition were shown to provide similar accuracy [12.30]. A freeware computer program, called *DSIFcalc* [12.31], is available for evaluating the results of impact tests using most of the methods mentioned above.

12.3.4 Ductile-to-Brittle Transition Region

The range of loading rates allowed by the ASTM E1921 standard [12.32] for a quasi-static evaluation is 0.1 to 2 MPa√m during the initial elastic portion. This range was drastically reduced from the previous version (2003), on account of recently published results [12.33] which demonstrate a strong influence of the loading rate on the reference temperature T_o measured according to the Master Curve methodology (Figure).

The current version of the standard (2005) does not include any provision for testing at higher loading rates, but work is currently in progress within the responsible ASTM sub-committee to prepare an Annex for higher loading rates, which should also include instrumented impact testing of precracked Charpy specimens.

The following empirical relationship allows quantifying the dependence of T_o from the loading rate [12.34]:

$$\Delta T_o = \frac{T_{o,st} \ln(\dot{K})}{\Gamma - \ln(\dot{K})} \tag{12.6}$$

with:

$$\Gamma = 9.9 \cdot \exp\left[\left(\frac{T_{o,st}}{190}\right)^{1.66} + \left(\frac{\sigma_{ys}}{722}\right)^{1.09}\right] \quad (12.7)$$

where σ_{ys} is measured at $T_{o,st}$.

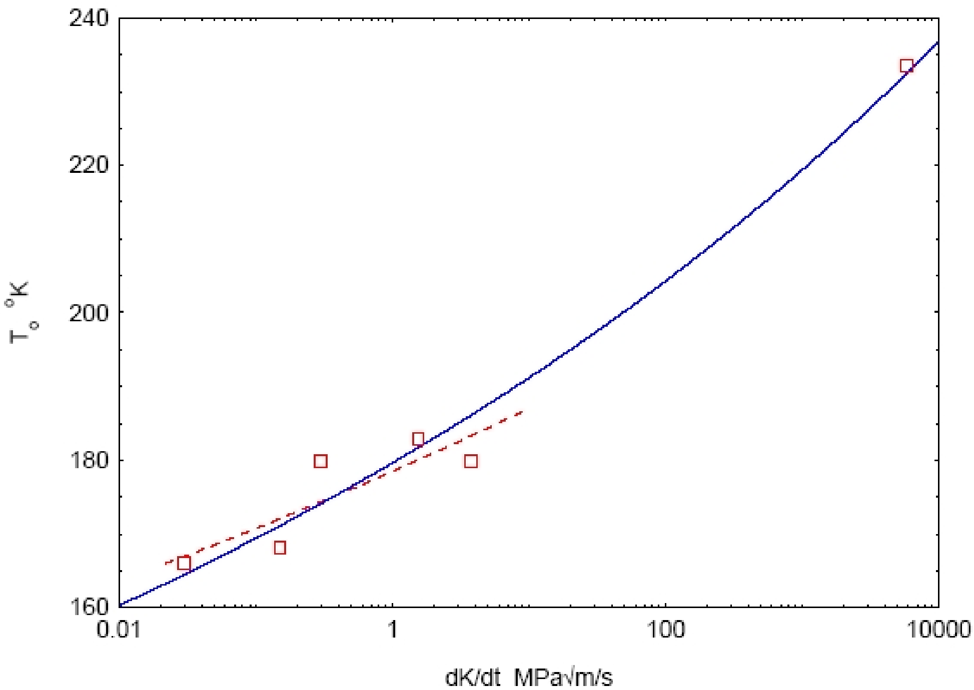

Figure 12.4 - Influence of loading rate on the reference temperature measured with ASTM E1921.

As far as the individual test results (J_c, K_{Jc}) are concerned, their determination generally does not differ from the quasi-static case since clevage fracture is expected to occur after a certain amount of plastic deformation and inertia effects are no more significantly affecting the force/displacement curve. This holds true even in the case of instrumented impact tests on precracked Charpy-type specimens, provided that impact speed does not exceed 1-1.5 m/s.

The determination of J-integral values in the case of rapid-load testing is also dealt with in Annex A14 of ASTM E1820, but since this Annex is more specific to fully ductile conditions, it will be described in more detail in the following section.

12.3.5 Upper Shelf (Fully Ductile Behaviour)

The quasi-static range prescribed by the ASTM E1820 standard is specified so that the time taken to reach the load P_f (defined in Annexes A1-A3 according to specimen geometry) lies between 0.1 and 10 min.

Special requirements for higher loading rates (rapid-load J-integral fracture toughness testing) are given in Annex A14. The most significant differences with respect to the quasi-static determination of the critical toughness (J_Q) and the crack resistance curve (J-R curve) are given below.

→ The force/displacement curve is analyzed to ensure that its initial portion is sufficiently well defined, so that an unambiguous J-R curve can be determined.

→ A minimum test time (t_w) is calculated from specimen stiffness and effective test mass. For test times less than t_w, a significant kinetic energy component is present in the specimen and the static J-integral equations are considered to be no more accurate.

→ For the evaluation of the crack resistance curve, the Normalization Data Reduction method described in Annex A15 is recommended. The elastic compliance method is not allowed. The multiple-specimen method can be used for evaluating the critical initiation toughness J_Q, but not for obtaining the J-R curve.

All other requirements and prescriptions for quasi-static testing remain applicable, including preparation of test specimens and validity criteria. Properties measured by rapid load testing must be denoted using in brackets the time needed to reach J_Q (J_Q(t), J_{Ic}(t), J-R(t) curve, etc).

The E1820 standard also mentions that "*the J-R(t) curve and J_{Ic}(t) properties are usually elevated by higher test rates*".

As for the ISO 12135:2002 standard, tests are limited to a maximum loading rate of 3 MPa√m/s in the linear elastic region and no indications for higher loading rate tests are given.

In case precracked Charpy-type specimens are impact tested in the fully ductile regime, the reference approach is the multiple-specimen method, where a series of nominally identical specimens are loaded up to selected displacement levels, resulting in corresponding amounts of stable crack extension. The resistance curve thus obtained is then analysed in accordance with the preferred test standard (ASTM E1820 or ISO 12135).

Variable amounts of ductile crack extension may be achieved using one of the following methods.

a) Low-Blow Test – This is the most popular method, and consists in limiting the impact velocity (and therefore the available energy) so that the specimen is not fully broken. Small differences between impact velocities for a specimen set are ignored.

b) Stop Block Test – The movement of the striker is arrested before the specimen is fully broken. The striker arrest position is varied from specimen to specimen.

c) Cleavage R-curve Method – For steels that exhibit brittle-to-ductile transition, the test temperature may be varied within the transition region in order to achieve different values of stable crack extension preceding cleavage. Small differences between test temperatures for a specimen set are ignored.

For any of these methods, the J-integral is calculated from the force/deflection record using the quasi-static formulas.

As an alternative to the multiple-specimen approach, single-specimen techniques have also been successfully applied for obtaining both critical toughness and crack resistance curves. The most commonly used is the Normalization Data Reduction Technique described in Annex A15 of E1820. This method [12.35] allows obtaining a J-R curve directly from the force/deflection record, using the initial and final crack measurements taken from the specimen surface, and cannot be applied if the specimen is fully broken (i.e. no final crack size can be measured). As a consequence, it can only be used in conjunction with the Low-Blow or Stop Block test procedure.

In addition, the ESIS TC5 Draft test method [12.25] reports a Key Curve approach [12.36,12.37] which allows estimating the J-R curve from a continuous force/deflection diagram as a function of Δa. This formulations only requires three parameters: F_{gy}, W_{mp} and W_t, as well as the specimen dimensional measurements. It can be used for both unbroken and fully broken specimens.

In a recent study [12.38], both the Normalization and the Key Curve method have been found in satisfactory agreement with the results of multiple-specimen (Low-Blow) tests, for two reactor pressure vessel steels with significantly different mechanical properties.

Given that, as shown above, an increase in loading rate causes an increase in fracture toughness in case of fully ductile behaviour, the use of quasi-static upper shelf toughness properties (J_{Ic}, J-R curve) in a dynamic situation always results in a conservative assessment.

12.3.6 Use of Dynamic Tensile Properties

For the analysis of fracture toughness tests, tensile properties measured at test relevant conditions (temperature and strain rate) have to be used.

In the case of high loading rate fracture toughness tests, the following options, listed in order of increasing accuracy, are available.

→ The use of quasi-static tensile properties (lower than dynamic values) is normally conservative, in that validity criteria (K_{limit}, J_{limit}, J_{max}) are proportional to σ_{ys} or σ_{flow}. However, in the upper shelf region the slope of the construction line used for measuring ductile initiation is proportional to σ_{flow} (ASTM) or σ_{UTS} (ISO), and therefore using quasi-static (lower) tensile properties delivers higher (non-conservative) critical values[1,2].

→ Dynamic yield strength values can be estimated from the force/deflection record of a Charpy test (V-notched or precracked) by using F_{gy} in analytical formulas obtained from Finite Element analyses [12.39].

→ Tensile properties at strain rates relevant to a Charpy test can be directly measured by performing high rate tensile tests. Although no official standard is available, a test procedure developed within ESIS TC5 has been issued as ESIS P7-00 [12.40].

12.3.7 Nomenclature

F_{gy} force at general yield in an instrumented Charpy test (kN)

J_c J-integral value at cleavage instability (kN/m²)

J_{Ic} initiation of ductile crack extension for quasi-static loading rates (kN/m²)

J_{Id} initiation of ductile crack extension for high (dynamic) loading rates (kN/m²)

J_{limit} validity limit for the determination of the J-R curve according to ASTM E1820 (kN/m²)

J_{max} validity limit for the determination of the J-R curve according to ISO 12135 (kN/m²)

---

[1] For impact tested precracked Charpy specimens, the ESIS TC5 draft [12.25] provides an analytical formula for estimating the construction (blunting) line in case the dynamic tensile strength is not available.

[2] The ASTM 1820 standard (Annex A13, eq.A13.2) provides a formula for estimating the dynamic yield strength of constructional steels having room temperature yield strengths below 480 MPa.

J_Q provisional value of J_{Ic} or J_{Id} (kN/m²)

K_{Ic} plane-strain fracture toughness for quasi-static loading rates (MPa√m)

K_{Id} plane-strain fracture toughness for high (dynamic) loading rates (MPa√m)

K_{Jc} stress intensity factor value at cleavage instability, calculated from J_c (MPa√m)

K_{limit} maximum measuring capacity of a specimen according to ASTM E1921 (MPa√m)

K_Q provisional value of K_{Ic} or K_{Id}, corresponding to the force P_Q (MPa√m)

$\dot{K}$ loading rate, expressed in terms of increase of stress intensity factor (MPa√m/s)

P_Q force value used to determine K_{Ic} or K_{Id} (kN)

t test time corresponding to the time needed to reach P_Q in a rapid-load plane-strain fracture toughness test according to ASTM E399 Annex A7 (ms)

t_f time to fracture used in the Impact Response Curve method (μs)

t_w minimum test time prescribed by ASTM E1820 for rapid-load J-integral fracture toughness testing (ms)

$T_{o,dyn}$ reference temperature for high (dynamic) loading rates, corresponding to a median toughness of 100 MPa√m for 1TC(T) specimens (°C)

$T_{o,st}$ reference temperature for quasi-static loading rates, corresponding to a median toughness of 100 MPa√m for 1TC(T) specimens (°C)

W_{mp} plastic component of the absorbed energy up to maximum force in an instrumented Charpy test (J)

W_t total absorbed energy in an instrumented Charpy test (J)

Δa crack extension (mm)

ΔT_o increase of reference temperature due to an increase in loading rate (°C)

σ_{ys} quasi-static yield strength (MPa)

σ_{flow} flow strength, calculated as the average of the yield and the ultimate tensile strengths (MPa)

12.3.8 Bibliography

[12.21] BS 7448-3:2005 Fracture mechanics toughness tests. Part 3: Method for determination of fracture toughness of metallic materials at rates of increase in stress intensity factor greater than 3.0 MPa√m/s, BSI London, 2005.

[12.22] ASTM E399, *Standard Test Method for Linear-Elastic Plane-Strain Fracture Toughness K_{Ic} of Metallic Materials*, Annual Book of ASTM Standards, Volume 03.01 (current edition: 2005).

[12.23] ASTM E1820, *Standard Test Method for Measurement of Fracture Toughness*, Annual Book of ASTM Standards, Volume 03.01 (current edition: 2001).

[12.24] ISO 12135, *Metallic materials - Unified method of test for the determination of quasistatic fracture toughness*, International Standard (current edition: 2002).

[12.25] ESIS TC5, *Proposed standard methods f or instrumented pre-cracked Charpy impact testing of steels*, Draft 15: April 2005.

[12.26] J.F. Kalthoff, S. Winckler and W. Böhme, *A Novel Procedure for Measuring the Impact Fracture Toughness K_{Id} with Pre-cracked Charpy Specimens*, Journal de Physique, Coll. C5, Suppl. No. 8, Tome 46, pp. 179-186, 1985.

[12.27] W. Böhme, *Dynamic Key Curves for Brittle Fracture Impact Tests and Establishment of a Transition Time*, ASTM STP 1074, J.P. Gudas, J.A. Joyce and E.M. Hackett, Eds., ASTM, Philadelphia, pp.144-156, 1990.

[12.28] H.J. McGillivray and D.F. Cannon, *The Development of Standard Methods for Determining the Dynamic Fracture Toughness of Metallic Materials*, ASTM STP 1130, R. Chona and W. Corwin, Eds., ASTM, Philadelphia, pp.161-179, 1992.

[12.29] J. Giovanola, *One-point-bend test*, Metals Handbook, Vol.8, American Society of Metals, Metals Park, pp.271-276, 1985.

[12.30] I.V. Rokach, *Modal approach for processing one- and three-point bend test data for DSIF-time diagram determination*. Fatigue & Fracture of Engineering Materials & Structures, **21**(8), 1007-1026, 1998.

[12.31] *DSIFcalc - free computer program for impact test data analysis*, available from: www.tu.kielce.pl/~rokach/dsifcalc.htm.

[12.32] ASTM E1921, *Standard Test Method for Determination of Reference Temperature, T_o, for Ferritic Steels in the Transition Range*, Annual Book of ASTM Standards, Volume 03.01 (current edition: 2005).

[12.33] J.B. Hall, and K.K. Yoon, *Quasi-static Loading Rate Effect on the Master Curve Reference Temperature of Ferritic Steels and Implications*, Proceedings of the 2003 ASME Pressure Vessels and Piping Conference, July 28-31, 2003, Cleveland.

[12.34] K. Wallin, *Effect of Strain Rate on the Fracture Toughness Reference Temperature T_o for Ferritic Steels*, "Recent Advances in Fracture", R.K. Mahidhara, et al., Eds., The Minerals, Metals & Materials Society, 1997.

[12.35] J.A. Joyce, *Analysis of the E08.02 High Rate Round Robin*, Journal of Testing and Evaluation, JTEVA, Vol. 29, No. 4, July 2001, pp. 329-351.

[12.36] H.J. Schindler, *Estimation of the Dynamic J-R Curve from a Single Impact Bending Test*, Proceedings of the 11th European Conference on Fracture, ECF11, Poitiers, 1996, EMAS Publ., pp. 2007-2012.

[12.37] H.J. Schindler, *Relation Between FractureToughness and Charpy Fracture Energy: an Analytical Approach*, ASTM STP 1380, T. Siewert and M.P. Manahan, Sr., Eds., ASTM, West Conshohocken, PA, 1999, pp. 337-353.

[12.38] E. Lucon, *Use of Single-Specimen Techniques for Measuring Upper Shelf Toughness Properties Under Impact Loading Rates*, SCK•CEN Report BLG-1016, September 2005.

[12.39] W.L. Server, *General Yielding of Charpy V-Notch and Precracked Charpy Specimens*, Journal of Engineering Materials and Technology, April 1978, Vol.100, pp. 183-188.

[12.40] ESIS P7-00, *ESIS Procedure for Dynamic Tensile Tests*, available at: http://ww www.esisweb.org/documents/Practice/practice.htm

12.4 Bi-modal Master Curve

12.4.1 Introduction

The basic Master Curve (MC) method for analysis of brittle fracture test results as defined in ASTM E1921-05 is intended for macroscopically homogeneous ferritic steels only. In reality, structural steels and their welds often contain inhomogeneities that distort the standard MC analysis. The inhomogeneity may be deterministic or random (or a mixture of both) in nature. Deterministic inhomogeneity, e.g. different fracture toughness at plate center and close to surface, can be accounted for provided that the specimen extraction histories are known and enough specimens are tested. Random inhomogeneity is somewhat more difficult to handle.

Since the standard MC analysis is merely applicable to homogeneous data sets, its use on a severely inhomogeneous data set can result in a clearly non-conservative description of the material. The MML estimation method (MML Stage 2 or Stage 3) in section 5.4.5.1 enables conservative lower bound types of fracture toughness estimates also for inhomogeneous material, in which case these estimates describe the fracture toughness of the more brittle constituent. Neither the MML analysis, nor standard MC analysis, can provide any information of the more ductile constituent. Therefore, a probabilistic description of the complete material is not possible. The bi-modal MC analysis method extends the standard MC analysis by describing the fracture toughness distribution of inhomogeneous material as the combination of two separate MC distributions. Thus, the bi-modal MC analysis method is particularly efficient in describing e.g. weld heat-affected zone (HAZ) data.

12.4.2 Principles of Bi-Modal Master Curve Analysis Method

In the case when the data population of a material consists of two combined MC distributions, the total cumulative probability distribution can be expressed as a bi-modal distribution of the form:

$$P_f = 1 - p_a \cdot \exp\left\{ -\left(\frac{K_{JC} - K_{\min}}{K_{01} - K_{\min}} \right)^4 \right\} - (1 - p_a) \cdot \exp\left\{ -\left(\frac{K_{JC} - K_{\min}}{K_{02} - K_{\min}} \right)^4 \right\} \tag{12.8}$$

where K_{01} and K_{02} are the characteristic toughness values for the two constituents and p_a is the probability of the toughness belonging to distribution 1. In the case of multi-temperature data, the characteristic toughness (K_{01} and K_{02}) is expressed in terms of the MC transition temperature (T_{01} and T_{02}). In contrast to a standard MC analysis where only one parameter needs to be determined, the bi-modal distribution contains three parameters. Thus, the fitting algorithm is somewhat more complicated than in the case of the standard MC or the MML lower tail estimation. In order to be able to handle randomly censored multi-temperature data sets, the estimation must be based on the maximum likelihood procedure.

The likelihood is expressed as:

$$L = \prod_{i=1}^{n} f_{ci}^{\delta_i} \cdot S_{ci}^{1-\delta_i} \tag{12.9}$$

where f_c is the probability density function, S_c is the survival function and δ is the censoring parameter.

The probability density function has the form (Eq. 3):

$$f_c = 4 \cdot p_a \cdot \frac{\left(K_{JC} - K_{\min}\right)^3}{\left(K_{01} - K_{\min}\right)^4} \exp\left\{-\left(\frac{K_{JC} - K_{\min}}{K_{01} - K_{\min}}\right)^4\right\} + 4 \cdot \left(1 - p_a\right) \cdot \frac{\left(K_{JC} - K_{\min}\right)^3}{\left(K_{02} - K_{\min}\right)^4} \cdot \exp\left\{-\left(\frac{K_{JC} - K_{\min}}{K_{02} - K_{\min}}\right)^4\right\} \quad (12.10)$$

and the survival function has the form:

$$S_c = p_a \cdot \exp\left\{-\left(\frac{K_{JC} - K_{\min}}{K_{01} - K_{\min}}\right)^4\right\} + \left(1 - p_a\right) \cdot \exp\left\{-\left(\frac{K_{JC} - K_{\min}}{K_{02} - K_{\min}}\right)^4\right\} \quad (12.11)$$

The parameters are solved so as to maximise the likelihood given by Eq. 2. The numerical iterative process is simplified by taking the logarithm of the likelihood so that a summation equation is obtained (Eq. 5).

$$\ln L = \sum_{i=1}^{n} \left[\delta_i \cdot \ln\left(f_{ci}\right) + \left(1 - \delta_i\right) \cdot \ln\left(S_{ci}\right)\right] \quad (12.12)$$

The bi-modal distribution model was found [12.41,12.42] to describe successfully fracture toughness data sets from the HAZs that generally exhibit substantial microstructural inhomogeneity. This is especially the case with multipass weldments containing local brittle zones (LBZ). Analyses of HAZ data sets revealed [12.41,12.42] that the MML analysis does not yield quite as conservative estimates of the lower bound toughness as the bi-modal distribution analysis. The bi-modal distribution recognises both the toughness of the more brittle constituent, as well as the amount of it, and can therefore be used to estimate the actual distribution or a hypothetical distribution consisting entirely of brittle material. The MML method gives an estimate that is mainly affected by the amount of the more brittle constituent. If this amount is small, the estimate will be influenced by the toughness of the tougher constituent.

In general, the MML method is intended for the analysis of small data sets, where the uncertainty related to size of the data set becomes an important factor. MML analysis is awaited to provide representative lower bound estimates suitable for structural integrity analysis purposes. Thus, the MML method should not be used e.g. to determine transition temperature shifts or in cases where the average fracture toughness is of interest.

The use of the bi-modal MC distribution should be focused on data sets of a sufficient size to provide information about the underlying material inhomogeneity. The bi-modal fit to the data can, as such, be very good, but a small data set may not describe the true distribution very accurately. The accuracy of the estimated parameters will depend on the data set size, occurrence probability (i.e., probability of hitting the different zones) and degree of censoring. Investigation on the accuracy of the bi-modal MC by performing a simple Monte Carlo simulation demonstrated that the standard deviation of the more brittle material can be approximated by Eq. 6, the more ductile material by Eq. 7 and the probability of occurrence of the more brittle material by Eq. 8.

$$\sigma T_{01} \approx \frac{22°C}{\sqrt{n \cdot p_a - 2}} \quad (12.13)$$

$$\sigma T_{02} \approx \frac{16°C}{\sqrt{r - n \cdot p_a - 2}} \quad (12.14)$$

$$\sigma p_a \approx \frac{0.35}{\sqrt{n \cdot p_a - 2}} \qquad (12.15)$$

Note that *n* is the total number of results and *r* is the number of non-censored results. If in any of the equations, the denominator becomes less than 1, the bi-modal estimate of the parameter in question should not be used. Eqs. 6-8 can also be used to judge the likelihood that the data represents an inhomogeneous material. A simple criterion can be expressed:

$$\left|T_{01} - T_{02}\right| > 2 \cdot \sqrt{\sigma T_{01}^2 + \sigma T_{02}^2} \qquad (12.16)$$

Any material fulfilling the criterion c.f. Eq. 9 is likely to be significantly inhomogeneous. The bi-modal MC estimate for inhomogeneous material should preferably be used with larger data sets than allowed for the basic MC or MML. The minimum data set size to be used with the bi-modal distribution is around 12-15, but, preferably, greater than 20. Smaller data sets do not describe the distribution sufficiently well to allow a confident estimation of the inhomogeneity.

12.4.3 Bibliography

[12.41] Wallin K, Nevasmaa P, Laukkanen A and Planman T: ‘Master Curve Analysis of Inhomoge- neous Ferritic Steels’. *Engineering Fracture Mechanics* **71** (2004). pp. 2329-2346.

[12.42] Nevasmaa P, Laukkanen A, Planman T and Wallin K: ‘A Novel Method for Fracture Toughness Assessment of Inhomogeneous Ferritic Steel Weldments using Bimodal Master Curve Analysis’. Proceedings of the ”*11th International Conference on Fracture (ICF XI)*”, Turin, 20-25 March 2005. The European Structural Integrity Society (ESIS) / Department of Structural Engineering and Geotechnics of the Politecnico di Torino. Topic 39, Paper ID No 4240. 6 p. (CD-ROM)

12.5 Treatment of non-sharp defects

12.5.1 Introduction

There are many situations where the defects that are, or might be, responsible for structural failure are not necessarily sharp. If defects are blunt it is overly conservative to proceed on the assumption that the defects behave like sharp cracks, coupled with the use of the sharp crack methodology. Components with non-sharp defects or notches exhibit an apparent fracture toughness that is greater than that obtained in cracked components because of a loss of constraint at the notch tip.

12.5.2 Stress distribution at notches

For brittle fracture of a sharp crack, fracture mechanics establishes that the critical situation is achieved when the applied stress multiplied by the square root of the crack length is equal to a constant [12.43]

$$\sigma^{c}\sqrt{a} = \text{constant}_1 \qquad (12.17)$$

where σ^c is the critical applied stress and a is the crack length. However, notches subject components to less critical situations in such a way that expression (12.17) becomes:

$$\sigma^{c} a^{\alpha} = \text{constant}_2 \qquad (12.18)$$

where α is a constant.

If the stress distribution at a notch tip is represented in the bi-logarithmic plot of Fig.12.5, three regions can be distinguished. Region I corresponds to a nearly constant stress zone, region II is a transition zone and region III is a zone where stresses follow the expression:

$$\sigma_{yy} = \frac{K_{\rho}}{(2\pi r)^{\alpha}} \qquad (12.19)$$

where K_ρ is the notch stress intensity factor.

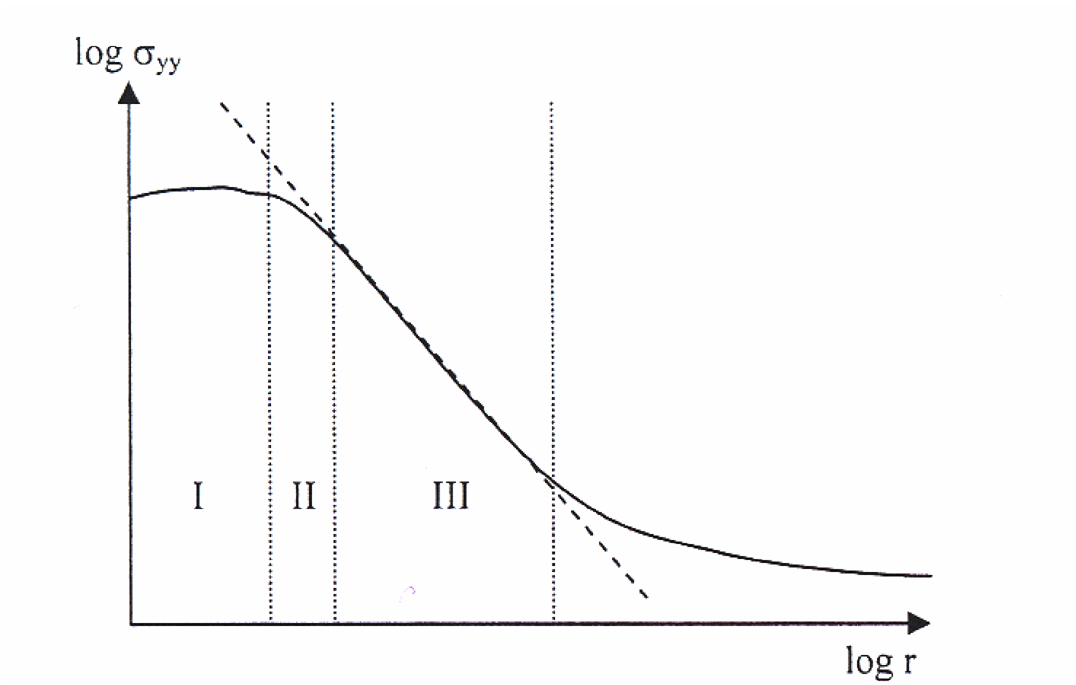

Figure 12.5 Bi-logarithmic graph of the stress distribution at a notch tip

12.5.3 Failure Criteria

There are two main failure criteria in notch theory: the global fracture criterion and the local fracture criterion [12.44]. The global criterion establishes that failure occurs when the notch stress intensity factor reaches a critical value:

$$K_{\rho} = K_{\rho}^{c} \tag{12.20}$$

On the other hand, one of the most extended local criteria is the critical average stress model [12.45, 12.46] which establishes that fracture propagates when the average stress within the effective distance, X_{ef}, is greater that the material strength, σ_f:

$$\frac{1}{X_{ef}} \int_{0}^{X_{ef}} \sigma(r) dr = \sigma_{f} \tag{12.21}$$

The effective distance corresponds to the point with lower stress gradient and needs finite element analysis for its determination

The critical average stress model has been used by Kim et al [12.47] to obtain the relation between the apparent fracture toughness K_{IN} developed by notched components and the fracture toughness obtained from deeply cracked specimens. Assuming the Creager and Paris [12.48] stress distribution at the notch tip, which is equal to that at a crack tip but displaced by a distance equal to $\rho/2$ along the x-axis, the expression along the θ=0° direction leads to:

$$\sigma_{yy} = \frac{K_I}{\sqrt{\pi(2r' + \rho)}}\left(1 + \frac{\rho}{2r'}\right) \tag{12.22}$$

where r' is the distance from the origin (located at the notch tip) to the point being assessed.

This expression is similar to that for cracks

$$\sigma_{yy} = \frac{K_I}{\sqrt{2\pi r}} \tag{12.23}$$

Equations (12.22) and (12.23) can be separately introduced in equation (12.21) and leads to the relation between K_{IN} and K_{IC}:

$$\frac{K_{IN}}{K_{IC}} = \sqrt{1 + \frac{\rho}{2X_{ef}}} \tag{12.24}$$

Equation (12.24) gives acceptable results and has been widely validated. However, from a practical point of view it has a problem: the need for finite element analysis to obtain X_{ef}.

Another relation between K_{IN} and K_{IC} is derived from so-called Finite Fracture Mechanics (FFM), developed by Taylor et al [12.49]. FFM is based on the Griffith theory [12.43] but considers that crack extensions are finite, Δa, instead of the differential equations assumed by Griffith. Moreover, Δa is a constant for a given material and failure mode. Summarising, this leads to the following equations:

$$K_{IN} = K_{IC}\sqrt{\frac{1}{1 - \frac{\rho}{10.04\,\Delta a}}} \qquad \text{(sharp notch solution)} \tag{12.25}$$

$$K_{IN} = K_{IC}\frac{1}{2.24}\sqrt{\frac{2\rho}{\Delta a}} \qquad \text{(blunt notch solution)} \tag{12.26}$$

The method given in [12.49] provides a criterion to determine which of equations (12.25) and (12.26) should be used in the case being studied.

Δa follows equation (12.27):

$$\Delta a = \frac{2K_{IC}^2}{\pi\sigma_{fl}^2} \tag{12.27}$$

When plasticity is confined to a very small region at the notch (ceramics and fatigue in metals) σ_{fl} is equal to the tensile strength, σ_u. For situations with more widespread plasticity σ_{fl} has to be calibrated and for brittle fracture of metals, σ_{fl} has been proposed to be $4\sigma_u$.

Finally, Spink et al. [12.50] have proposed that for semi-elliptical notches:

$$K_{IN} = \frac{K_{IC} + \sigma_u(\pi\rho)^{1/2}}{1 + \sqrt{\left(\frac{\rho}{c}\right)}} \tag{12.28}$$

where c is the semi-major axis.

It is important to note that these methods are derived from LEFM and will not be applicable to failures by ductile mechanisms.

12.5.4 Flaws at the tip of a notch

There are no generalised solutions available for flaws situated at notch tips. In general, such flaws may be assessed conservatively by using standard solutions and assuming the total depth is equal to the sum of the depths of the flaw and the notch. An assessment of this type is satisfactory for flaws associated with sharp notches but may be unnecessarily conservative for blunt notches. In such cases, standard solutions for the depth of the flaw alone may be multiplied by the stress concentration factor of the notch, or, where a stress analysis may be performed, the stress gradient due to the notch may be allowed for.

It should be noted that very short flaws at the tip of very sharp notches may require special attention because of localised plasticity effects.

It is proposed that the "modified RSM" methodology [12.51] should be used for determining the J integral for a flaw at the edge of a notch. It combines the EPRI and RSM estimation schemes and provides the following equation for J which may be applied at all levels of crack tip plasticity, from the linear elastic to the fully plastic limit, and for all crack depths:

$$J = J_e\,(d+\Phi^* r_y)+J_e(d).[E\varepsilon^p_{ref} / \sigma_{ref}] \tag{12.29}$$

where d is the crack length, $\sigma_{ref}=P/P^*_L$, $\varepsilon^p_{ref} = \alpha'\ (P/P^*_L)^n$, P^*_L is an estimated yield load for the cracked structure often approximated by P_L, based on the remaining uncracked section, α' is the coefficient in the Ramberg-Osgood law (not the constraint parameter) and Φ^2 and r_y are evaluated according to the following equations:

$$\Phi^* = [1+(P/P^*_L)^2]^{-1} \tag{12.30}$$

$r_y = (1/\lambda\pi).(n-1/n+1).(K/\sigma_0)^2$ (12.31)

Where λ=2 for plane stress and 6 for plane strain. n is the exponent in the Ramberg-Osgood law. The FAD is then constructed from:

$K_r = [J_e\,(d,P) / J\,(d,P)\,]^{0.5}$ (12.32)

$L_r = P / P_L\,(a/b)$ (12.33)

12.5.5 Failure Assessment Diagram For Notches

A simple methodology is shown below that allows for the assessment of components with low constraint due to not only shallow defects or tensile loading but also to notch-type defects, that is, a procedure that provides a global treatment for the in-plane loss of constraint.

The method suggests that both losses of constraint are independent. Therefore, using the modified FAD procedure and the critical average stress model from equation (12.24), the assessment of a component with a shallow notch and subjected to tensile loading is performed using the following equation for the modified FAD:

$$K_r = f(L_r).(1+\alpha(-\beta L_r)^k)\sqrt{1+\frac{\rho}{2X_{ef}}} \qquad L_r \le L_r^{\max} \qquad (12.34)$$

The independence of both phenomena is justified [12.52, 12.53] by applying the critical average stress model and the Creager distribution (as Kim et al did [12.47]), considering not only the first term in William's series, but also the second term (T-stress). Because the T-stress is a constant and not a function of distance from the crack/notch tip, if the stress distribution in a crack is displaced ρ/2 as Creager did in order to obtain the stress distribution in a notch, the T-stress does not change.

12.5.6 Bibliography

[12.43] Griffith A.A., 1920, "The phenomena of rupture and flow in solids", Phil. Trans. R. Soc. London. A 221, pp.163-198

[12.44] Pluvinage G., 1998, "Fatigue and fracture emanating from notch; the use of the notch stress intensity factor", Nuclear Engineering and Design, 185, pp.173-184

[12.45] Bao Y., Jin Z., 1993, Fatigue Fract. Eng. Mater. Struct., 16, 829

[12.46] Fenghui W., 2000, Journal of Material Science, 35, 2534

[12.47] Kim JH, Kim DH, Moon SI, 2004, "Evaluation of static and dynamic fracture toughness using apparent fracture toughness of notched specimens", Materials Science and Engineering A, Volumes 387-389, 15 December 2004, pp. 381-384

[12.48] Creager M, Paris C., 1967, "Elastic field equations for blunt cracks with reference to stress corrosion cracking", International Journal of Fracture, 3, pp247-252

[12.49] Taylor D., Cornetti P and Pugno N., 2004, "The fracture mechanics of finite crack extension", Engineering Fracture Mechanics, v.72, N7, pp.1021-1038.

[12.50] Spink GM, Worthington PJ, Heald PT, "The effect of notch acuity on fracture toughness testing", Materials Science and Engineering, 11, 113-117, 1973

[12.51] McClung RC, Chell GG, Lee YG, Russell DA, Orient GE, 'Development of a practical methodology for elastic-plastic and fully plastic fatigue crack growth', NASA/CR-1999-209428 (1999)

[12.52] Cicero S., 2005, 'Evaluación de la integridad structural de componentes sometidos a condiciones de bajo confinamiento', PhD Thesis, University of Cantabria, Santander, Spain.

[12.53] Cicero,S., Gutiérrez-Solana, F., Álvarez, J.A., 'Structural Integrity Assessment of Components with Low Constraint, Proceedings of 16th European Conference of Fracture, Alexandropoulos, Greece, July 2006.